

---

---

# Diagnosis of Vibration Systems for Decision Making

**Noureddine HALOUI \***

*LASS, Electronics Department, University Mohamed Boudiaf of M'sila, Algeria,  
noureddine.haloui@univ-msila.dz*

**Mohamed LADJAL**

*LASS, Electronics Department, University Mohamed Boudiaf of M'sila, Algeria,  
mohamed.ladjal@univ-msila.dz*

**Thomas RODET**

*ENS Paris-Saclay, Paris-Saclay University, 91190 Gif-sur-Yvette, France,  
thomas.rodet@ens-paris-saclay.fr*

\* Author to whom correspondence should be addressed

*Abstract:* - Defect detection in mechanical systems is of critical importance in industrial applications, particularly for rotating components. This paper presents a model-based methodology for early online detection of mechanical faults using vibration analysis. The proposed approach is implemented in three main phases: model identification, optimal filter synthesis, and fault detection. A key advantage of this method is its ability to detect faults automatically, without requiring expert interpretation, and the possibility of putting it online or offline. This is achieved through a physics-based model of the system and an optimized implementation. Fault detection relies on analyzing the variance of the residual signal, defined as the difference between measured outputs and those estimated by the optimal filter. A fault is flagged when this variance exceeds a predefined threshold. The effectiveness of the method is demonstrated experimentally on a vibratory mechanical test bench equipped with gears. Validation is performed by comparing the results with expert assessments conducted during the experiments and with findings reported in the literature.

*Keywords:* - Vibration; fault diagnosis; optimal filter; gearboxes; model identification, decision coefficient.

---

## 1. INTRODUCTION

Fault detection and diagnosis in mechanical systems are essential to ensuring reliability, safety, and cost-effective maintenance, particularly in rotating machinery commonly found in transportation, automotive applications, and power transmission [1-3].

These systems are prone to mechanical failures, especially within motion transmission components such as gearboxes and shafts [4]. Traditional fault analysis techniques, often based on signal shape or frequency domain projections, are useful but inherently limited: they typically do not account for the dynamic behavior associated with evolving faults [5-10].

To overcome these limitations, model-based fault detection methods have gained prominence. These approaches rely on comparing measured input-output signals to those estimated by a dynamic model of the system, enabling more precise and early fault characterization [11], [12]. Among these, observer-based methods stand out for their ability to

generate residuals that reflect deviations between the actual and modeled system behavior and thus serve as indicators of abnormal operation [2], [4], [13].

Several techniques have been proposed for residual generation and evaluation, including linear and adaptive observers and, more recently, artificial intelligence methods. The growing interest in observer-based approaches underlines their robustness and effectiveness across a range of applications [11], [14-16].

In this study, we propose a novel observer-based methodology for real-time, online fault detection in vibratory systems. The main contributions of this work are as follows:

A decision-making criterion based on a decision coefficient  $C_{dd}$ , which is directly derived from the variance of the residual  $\sigma_r^2$ . A fault is detected when this variance exceeds a predefined threshold  $S_d$  eliminating the need for human interpretation:

$$C_{dd} = \begin{cases} 0 & \text{if } \sigma_r^2 < S_d \rightarrow \text{no fault} \\ 1 & \text{if } \sigma_r^2 \geq S_d \rightarrow \text{fault detected} \end{cases} \quad (1)$$

An entirely automatic detection strategy, grounded in physical modeling of the mechanical

system, that avoids the graphical analysis or spectral signature identification typically required by other methods, such as signal processing methods (temporal, frequency, and time-frequency methods) [17] [18] or data-guided methods (fuzzy logic, neural network methods) [19].

The use of an optimal filter after the model identification phase, which improves the accuracy of estimated outputs and enhances the sensitivity of the detection process.

Lastly, the resolution in frequency usually cannot make the distinction between the responses in the spectrum of two or more harmonics [9] [10] [20]. These performance limitations that are born by the FFT approach have elicited many modern parametric estimation techniques over the last two decades; however, the sensors cannot be placed directly on the rotating mechanical elements generally, the only possibility is to place them on their frames [13] [21]. Such a solution compromises the information associated with the failure of the rotating elements by various other information and noises unfavorable to the spectral analysis [22]. The model-based approach was applied successfully, which gave better results [16] [23-26].

This work is experimentally validated on a gear transmission test bench, chosen due to the mechanical importance and known vulnerability of such systems. While FFT remains a common diagnostic tool, our results demonstrate that the proposed model-based methodology yields more robust and interpretable fault detection, without relying on expert knowledge.

The paper is structured as follows: section 2 presents the identification process, dedicated to the choice the structure of model and the estimation of the parameters; section 3 details the synthesis of the optimal filter design for residual generation and decision-making mechanism; section 4 provides experimental validation results; section 5 comparative table of the proposed method with those of the state of the art and section 6 concludes the study with a discussion of the findings and future perspectives.

## 2. IDENTIFICATION

The model identification involves an autoregressive structure of order  $n$  is given by [24] [27].

$$y(k) = -\sum_{i=1}^n a_i y(k-i) + v(k) \quad \forall k \in \mathbb{N} \quad (2)$$

where all parameters  $a_i \in \mathbb{R}^*$ ,  $\{v(k)\}_{k \in \mathbb{N}}$  is white noise with variance  $\sigma_v^2$ , and  $\{y(k)\}_{k \in \mathbb{N}}$  is model output.

To choose the order of the model, we take into account the physical properties of the system. The fact that the signal has a periodic dominance means that the dimension of the model must recreate its setting for  $n = 2$ , which produces the frequency of the system, therefore:

$$y(k) = -a_1 y(k-1) - a_2 y(k-2) + v(k) \quad (3)$$

To determine the parameters  $a_1$  and  $a_2$  of model (3), we use the online autocorrelation  $R_{yy}(k)$  approach, where  $R_{yy}(k)$  is obtained from the measurements on the system [27].

$$R_{yy}(k) = \frac{1}{n-k} \sum_{i=1}^{n-k} y(i+k)y(i) \quad (4)$$

$y(i)$  is the known observation data for  $i = 1, 2, 3, \dots, n$ . The  $a_1$  and  $a_2$  are given respectively by [27]:

$$a_1 = -\frac{R_{yy}(1)}{R_{yy}(0)} \quad (5)$$

$$a_2 = \frac{[R_{yy}(2) + a_1 R_{yy}(1)]}{\sigma_{y_1}^2} \quad (6)$$

So :

$$\sigma_{y_1}^2 = (1 - |a_1|^2) \sigma_{y_0}^2$$

and

$$\sigma_{y_0}^2 = R_{yy}(0)$$

## 3. OPTIMAL FILTER SYNTHESIS

To maintain the overall consistency of the proposed approach, we use the Kalman filter in this step to obtain a good estimate of the system state [14], [15]. The objective is for the estimation error to be zero on average and of minimal variance. Let's consider the Kalman model in the discrete domain and assume that our system is perturbed.

$$\begin{cases} x(k) = A_d x(k-1) + w_d(k) \\ y(k) = C_d x(k) + v_d(k) \end{cases} \quad (7)$$

where  $x \in \mathbb{R}$  is the state vector,  $y \in \mathbb{R}$  is the measured output vector,  $w_d \in \mathbb{R}$  is the processed noise,  $v_d \in \mathbb{R}$  is the measurement noise.

Before deriving the Kalman filter that minimizes the estimation error and defines the fault indicator, equation (3) must first be consistent with model (7). The Z-transform (discrete-time equivalent representation) of model (3) is then obtained as follows;

$$H(z) = \frac{Y(z)}{V(z)} = \frac{1}{a_2 z^2 + a_1 z + 1} \quad (8)$$

To find the state representation of our mechanical system, characterized by its transfer function  $H(z)$  we use the canonical transformation, which gives:

$$A_d = \begin{bmatrix} 0 & 1 \\ -a_1 & -a_2 \end{bmatrix} \dots\dots\dots(9)$$

$$C_d = [1 \ 0] \dots\dots\dots(10)$$

To determine the synthesis algorithm and find a Kalman filter, we take into account that  $w_d$  is an unknown process noise due to many factors such as material, connection, and environment, with a known covariance  $W_d$ , moreover, the system measurement cannot be exactly accurate, and the measurement noise  $v_d$  is widely present in the real-time system model, with a known covariance  $V_d$ .

The interest in using the Kalman filter algorithm is to find the optimal estimate of the state of the system  $\hat{x}(k)$ ; this estimate is based on the dynamics of the system and the output measurement of the system with the noise  $y(k)$ .

The Kalman filter works in two phases: the first is the prediction phase, and the second is the update phase. Prediction phase: this is the evolution of the dynamic system over time, at time  $k$  we have an estimate which is based on the knowledge of all the measurements up to time  $k - 1$  which we note  $\hat{x}(k - 1)$ , without taking into account the measurement  $y(k)$ .

The second phase is the update of the estimated state from the measurement  $y(k)$  and the gain of the Kalman filter. These two phases allow us to determine the equations used to calculate the Kalman filter algorithm and to obtain the a posteriori estimate  $\hat{x}(k)$ .

### 3.1. Diagnostic procedure

This part of the proposed methodology establishes the fault-detection criterion. This step exploits the coherence between model identification and observation: if the system remains healthy, the measurements and the model estimations remain close; if a fault develops, their difference increases measurably.

After the model has been identified and the optimal Kalman filter synthesized, the state estimate  $\hat{x}(k)$  can be updated in real time using the measured output  $y(k)$ . The corresponding estimated output  $\hat{y}(k)$  is obtained as:

$$\hat{y}(k) = C_d \hat{x}(k) \dots\dots\dots(11)$$

where  $C_d$  is the output matrix is derived from the AR(3) model. The residual signal  $r(k)$  defined as the difference between the measured and estimated outputs:

$$r(k) = y(k) - \hat{y}(k) \quad (12)$$

By substituting equation (12) into equation (11), we obtain:

$$r(k) = y(k) - C_d \hat{x}(k) \quad (13)$$

In practice, at the initial instant, there is no measurement to determine the estimated state of the system, so it is logical to define the state of the a posteriori estimate as being equal to the a priori estimate.

To obtain information on the operating state of the mechanical system, plus the fault detection on the latter and its evolution over time, we use the calculation of the variance  $\sigma_r^2$  given by the following expression:

$$\sigma_r^2 = \sum_{k=1}^N (r(k) - \bar{r})^2 \dots\dots\dots(14)$$

With:  $\bar{r}$  is the average of the residues, which corresponds to a rotation period of the system.

The variations in  $\sigma_r^2$  over time, when exceeding a certain well-defined threshold ( $S_d$ ), translate into a failure, since this variation compensates for the model deviation caused by a fault in the mechanical system.

The choice of the technique used to determine the detection threshold  $S_d$  is a key step in the diagnostic procedure, as this threshold defines whether a fault is present or not. The value of  $S_d$  is obtained by multiplying the maximum residual variance estimated during a fault-free period,  $\sigma_{r^2 \max(sd)}$ , by a coefficient called the mechanical adaptation coefficient, denoted  $f_m$ .

This coefficient allows us to compensate for slight increases in the residual variance relative to the maximum variance estimated during the initial fault-free phase, thereby preventing false fault alarms during normal operation. In rotating mechanical systems, the released energy gradually increases over time due to several phenomena, such as the rise in lubricant temperature. These effects contribute to a minor increase in the residual variance, which must be taken into account.

Therefore, the coefficient  $f_m$  is defined as the ratio between the maximum estimated residual variance  $\sigma_{r^2 \max(sd)}$  and its average value  $\sigma_{r^2 \text{ moy}(sd)}$  during the fault-free start-up time, as expressed by:

$$f_m = \frac{\sigma_{r^2 \max(sd)}}{\sigma_{r^2 \text{ moy}(sd)}} \quad (15)$$

Accordingly, the detection threshold  $S_d$  is given by:

$$S_d = \sigma_{r^2 \max(sd)} \cdot f_m \quad (16)$$

In our gear test-bench application, the calculated value of the mechanical adaptation coefficient is  $f_m = 1.21$ .

Generally, the value of the fault detection threshold ( $S_d$ ) is between the maximum value of the variance calculated over a period during normal operation without a fault noted  $\sigma_r^2_{max(sd)}$  and the minimum value of the variance during operation with a fault noted  $\sigma_r^2_{min(ad)}$  with:

$$\sigma_r^2_{max(sd)} < S_d \leq \sigma_r^2_{min(ad)} \quad (17)$$

We can translate the value of the detection threshold  $S_d$  as precise information on the fault detection time, this value determines the value of the decision coefficient ( $C_{dd}$ ) defined by the expression (1) from the measurements.

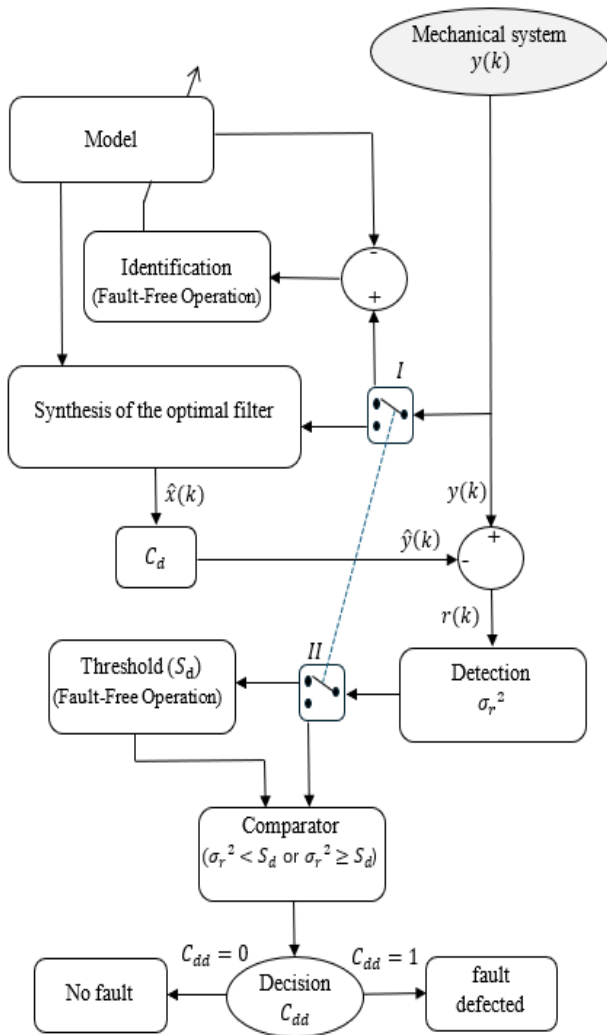


Figure 1. Procedure for fault detection

Therefore, the proposed approach to diagnose faults in mechanical systems can be summarized by Figure 1, which shows the different steps of the Kalman filter-based approach, using the comparison of the temporal variation of the estimation error variance  $\sigma_r^2$  with respect to the detection threshold  $S_d$  to determine the value of the decision coefficient  $C_{dd}$  according to expression (1).

## 4. PROBLEM FORMULATION TO TEST THE PROPOSED METHOD

The tests of the validity and effectiveness of the proposed approach are carried out on real gearbox data delivered by CETIM (Centre des Etudes Techniques des Industries Mécaniques de Senlis), along with an expert report shown in Table 1 [21] [28]. Signals were produced by a continuously operated gearbox system (figure 2), where the gear wheel sizes and operating parameters (speed, torque) were set so that spalling would occur across the entire width of a tooth.

Vibration signals were measured using an accelerometric sensor located on the gearbox input shaft. During the gearbox input shaft rotation, angular sampling, which implied taking  $p$  samples per revolution. The rotational position of the motor shaft was monitored by an optical incremental encoder directly fitted with the 1st shaft. This optical encoder gives a pulse train of  $p$  slots per revolution from the vibration signal is sampled.

The sensor output is a voltage that is proportional to the acceleration. It is then amplified by the charge amplifier and filtered to verify Shannon's theorem. The system would be stopped on a daily basis during experimentation to check the state of the wheel teeth and subsequently write the expertise report of Table 1. The system specifications are:

- The number of teeth is respectively 20 teeth on the first wheel apeled pinion and 21 teeth on the second wheel.
- $Rpm = 1000$  turns/min is the rotation speed of the input transmission, which induces a rotation frequency
- $f_r \approx 16.66$  Hz and 15.86 Hz for the input and output tree.
- $f_e \approx 333$  Hz is the meshing frequency.

Table 1. Expertise report [21]

Days	Observations
1	Nothing to report
2	// //
3	// //
4	// //
5	// //
6	Tooth spalling 1/2
7	No evolution
8	Tooth 1/2 no evolution, tooth 15/16 spalling beginning
9	Spalling evolution of tooth 15/16
10	// //
11	// //
12	Spalling on the entire width of tooth 15/16

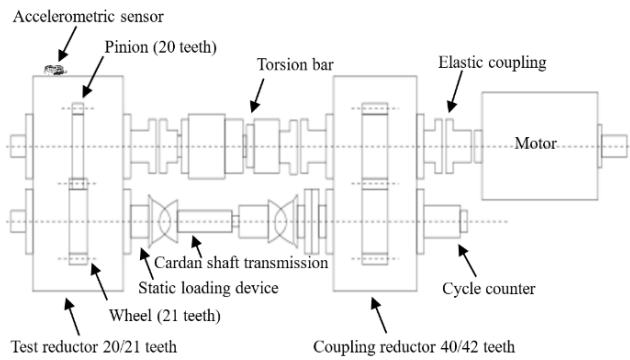


**Figure 2.** Representative diagram of a gearbox

The reductor system was kept running for 12 days continuously, and readings were taken once daily. Each reading comprises about 60000 samples, implying 50 rotation cycles at a sampling frequency of 20 kHz. The test setup is made to run from a healthy operating condition to a faulty one.

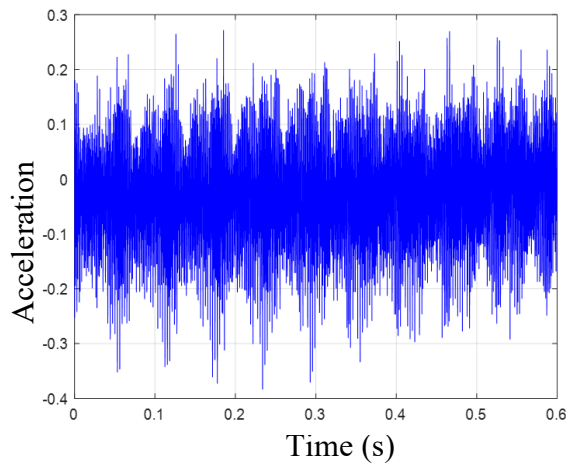


**Figure 3.** Temporal representation of the vibration signal

Vibration is taken as the prime physical quantity for studying the transmission of signals for gear health. These vibrations are generated primarily by the impacts between the wheel teeth in the transmission. The level of these impacts depends on the state of health of the teeth during normal healthy operation and the nature of the fault when the system is in a degraded state. The recorded vibrating signal (Figure 3) contains the information about the operating state of the gearbox.

This signal is quasi-periodical, and its meshing frequency is equal to the frequency of one of the wheels, multiplied by the number of teeth on the same wheel. This fact motivated the proposed model (3).

#### 4.1. Application to gear box fault-diagnosis

To detect the gear tooth defects, the concept of the methodology that has been proposed in the

previous sections (Figure 1), which consists of defining the second-order model and estimating these parameters, then synthesizing the Kalman filter in the second step, which finally, in the third step, allows for determining the variance of the estimation residual compared to the detection threshold ( $S_d$ ) to assign the decision coefficient ( $C_{dd}$ ) the value zero (no fault) or one (fault detection) is shown in Figure 4. The detection threshold ( $S_d$ ) is determined during the first day of operation of the system under the condition that no failure occurs.

The threshold value for detection  $S_d$  (16) equals the maximum value of the variance  $\sigma_r^2 \max(sd)$  of the estimation error over a rotation period, which is 1200 residual samples, this maximum variance value is to be multiplied by the mechanical adaptation coefficient  $f_m=1,21$  (15).

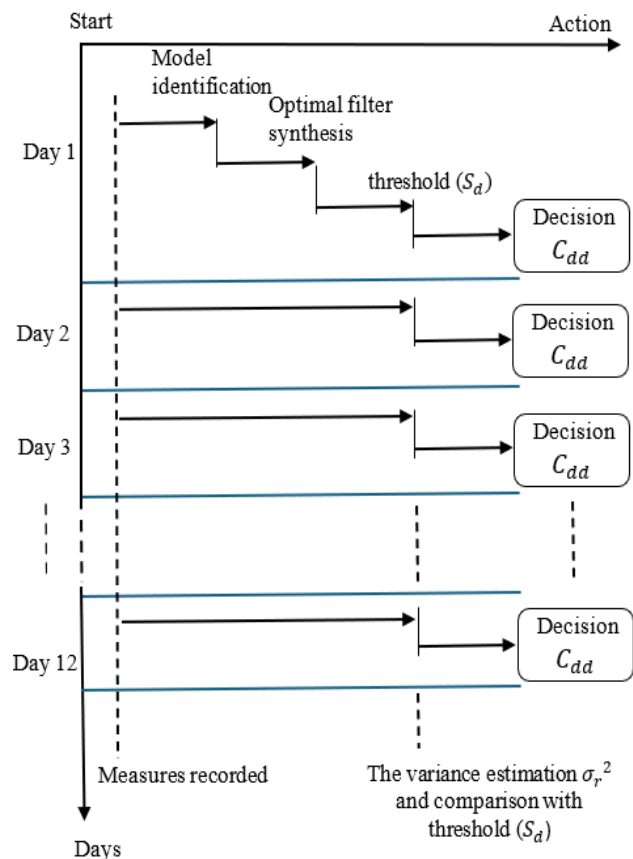


**Figure 4.** Application diagram of the method

Figure 5 clearly shows that the value of the detection threshold is equal to the variance of the estimation error corresponding to the fortieth period of the first day multiplied by  $f_m=1,21$ . Then, comparing the evolution of the variance of the estimation error (figure 5) during each day of operation of the system with respect to the detection threshold ( $S_d$ ) allows us to determine the value of the decision coefficient  $C_{dd}$  (figure 6). Note clearly in Figure 5 that the value of the detection threshold  $S_d$  corresponds to the value of the minimum

variance of the thirtieth period of the 6th day of operation of the system, which justifies the expression (17).

As shown in Figure 6, when the fault occurs on the 6th day, it is clearly observable without any knowledge of the behavior of the system.

It is clear that from the 6th day, the decision coefficient indicates the presence of a fault. This simplicity of diagnosis is made possible thanks to the model and the optimal Kalman filter implemented.

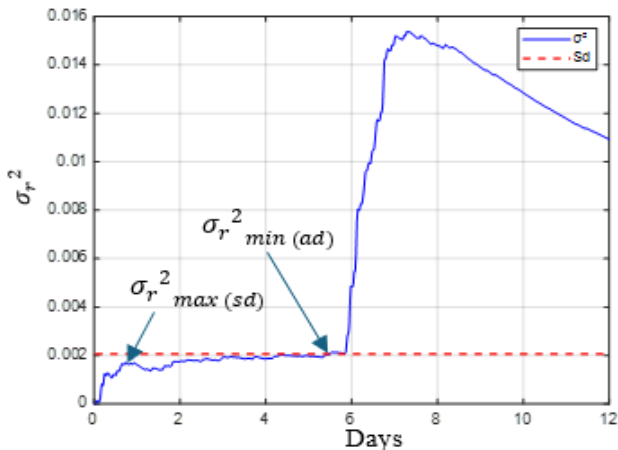


Figure 5. Daily evolution of  $\sigma_r^2$

Indeed, the identification of the model gives the dynamics of the system, and thus, the deviation induced by the fault will be directly observed on  $C_{dd}$  (Figure 6), without recourse to an expert.

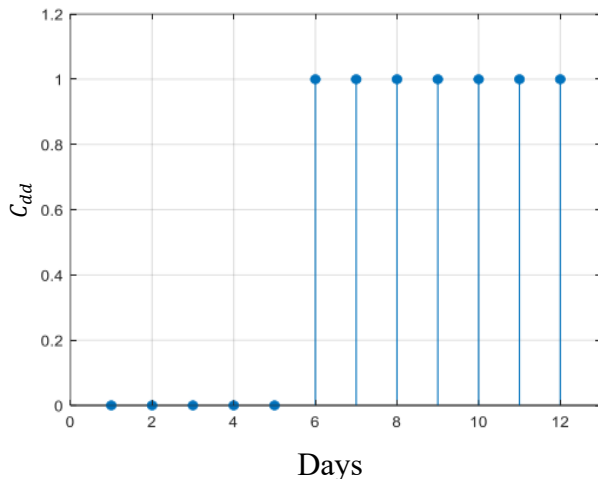


Figure 6. Daily evolution of the decision

This quality of diagnosis is due to the quality of the model identification and the robustness of the optimal filter. Thus, the limitation of the method is related to the quality of the identification, where it is assumed at this stage that the system is not affected by a failure. Thus, the assumption of the good health of the system must be verified at the identification stage, otherwise the method fails.

## 5. COMPARATIVE TABLE OF THE PROPOSED METHOD WITH THOSE OF THE STATE OF THE ART

The proposed method, based on optimal filtering, allows for the early detection of faults, both online and offline, without expert intervention.

In contrast, kurtosis analysis (Figure 7) and synchronous cepstrum analysis (Figure 8) based on the residual  $r$  (Figure 9), which is the difference between the amplitudes of the two peaks (wheel and pinion), do not allow for early detection, and the interpretation of the diagnostic results requires a specialist.

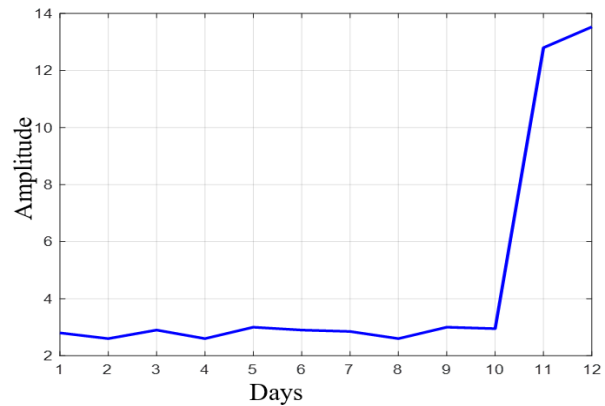


Figure 7. Kurtosis value of the acceleration signal [28,29]

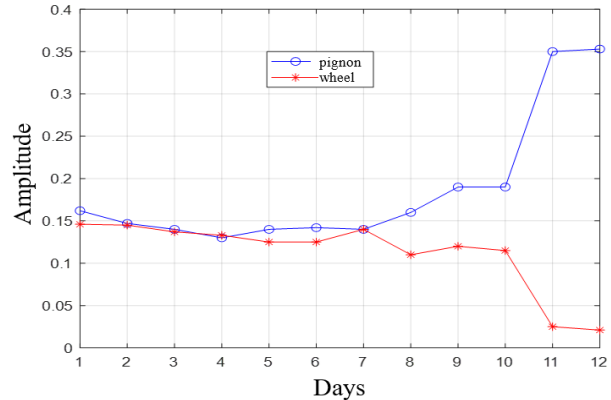


Figure 8. Evolution of synchronous cepstrum Peaks [21,30]

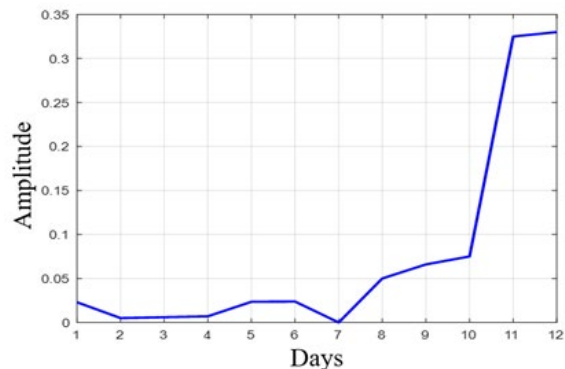


Figure 9. Evolution of the residue ( $r$ ) of synchronous cepstrum

Table 2 below summarizes the different comparison criteria between the proposed method based on optimal filtering and the most widely used state-of-the-art methods for detecting gearbox faults [21, 28-30].

**Table 2.** Comparative study of methods

Methods Criteria	Kurtosis analysis	Synchronous cepstrum analysis	Optimal filter
Complexity	No	No	No
Accuracy	No	No	Yes
Cost	Cheape	Cheape	Average
Ease of implementation	Yes	Yes	Yes
Early fault detection	No	No	Yes
Offline	Yes	Yes	Yes
Online	No	No	Yes

## 6. CONCLUSION

This work presents a model-based methodology for the early online detection of gear faults in rotating machines using optimal filtering. A key strength of the approach lies in its ability to detect failures automatically, without requiring expert interpretation or visual signature analysis. This is made possible by introducing a decision coefficient based on the variance of the residual, which transitions from 0 to 1 when a fault is detected. The use of a second-order stochastic model, combined with an optimal filter, provides a robust framework for distinguishing between healthy and faulty system states.

The limitation of this method is that it cannot be applied to a system that already has a fault.

The effectiveness of the method has been demonstrated through experiments on a vibratory gearbox system, where the detection criterion correlated well with expert assessments and published literature.

Unlike conventional techniques that rely on spectral signatures or manual interpretation, the proposed approach offers a simplified and automated solution by replacing the fault signature with a statistically defined decision threshold. This makes it particularly suitable for real-time applications in industrial environments.

The confidence in the method relies on the appropriate selection of the detection threshold, which ensures a good balance between sensitivity and robustness. Future work may focus on extending the approach to other types of mechanical systems.

## ACKNOWLEDGMENTS

The authors would like to thank the LASS, Laboratory of Signal and Systems Analysis, Department of Electronics, Faculty of Technology, University of M'sila, M'sila 28000, Algeria, and SATIE Laboratory, ENS, University of Paris-Saclay, France.

## REFERENCES

- [1] L. Zhao and Y. Chen, "Dynamics and Fault Diagnosis of Railway Vehicle Gearboxes: A Review," *Journal of Dynamics, Monitoring and Diagnostics*, vol. 3, no. 2, pp. 83–98, Jun. 2024, doi: 10.37965/jdmd.2024.518.
- [2] M. Frini, A. Soualhi, and M. El Badaoui, "Gear faults diagnosis based on the geometric indicators of electrical signals in three-phase induction motors," *Mech Mach Theory*, vol. 138, pp. 1–15, Aug. 2019, doi: 10.1016/j.mechmachtheory.2019.03.030.
- [3] S. Chen, Z. Liu, X. He, D. Zou, and D. Zhou, "Multi-mode fault diagnosis datasets of gearbox under variable working conditions," *Data Brief*, vol. 54, Jun. 2024, doi: 10.1016/j.dib.2024.110453.
- [4] K. F. Brethee, D. Zhen, F. Gu, and A. D. Ball, "Helical gear wear monitoring: Modelling and experimental validation," *Mech Mach Theory*, vol. 117, pp. 210–229, Nov. 2017, doi: 10.1016/j.mechmachtheory.2017.07.012.
- [5] M. El Badaoui, F. Guillet, and J. Danière, "New applications of the real cepstrum to gear signals, including definition of a robust fault indicator," *Mech Syst Signal Process*, vol. 18, no. 5, pp. 1031–1046, 2004, doi: 10.1016/j.ymsp.2004.01.005.
- [6] J. Yao, C. Liu, K. Song, C. Feng, and D. Jiang, "Fault diagnosis of planetary gearbox based on acoustic signals," *Applied Acoustics*, vol. 181, Oct. 2021, doi: 10.1016/j.apacoust.2021.108151.
- [7] F. Chaari, W. Bartelmus, R. Zimroz, T. Fakhfakh, and M. Haddar, "Gearbox vibration signal amplitude and frequency modulation," *Shock and Vibration*, vol. 19, no. 4, pp. 635–652, 2012, doi: 10.3233/SAV-2011-0656.
- [8] T. Du Nguyen and P. D. Nguyen, "Improvements in the Wavelet Transform and Its Variations: Concepts and Applications in Diagnosing Gearbox in Non-Stationary Conditions," *Applied Sciences (Switzerland)*, vol. 14, no. 11, Jun. 2024, doi: 10.3390/app14114642.
- [9] N. H. Chandra and A. S. Sekhar, "Fault detection in rotor bearing systems using time frequency techniques," *Mech Syst Signal Process*, vol. 72–73, pp. 105–133, May 2016, doi: 10.1016/j.ymsp.2015.11.013.
- [10] Z. Feng and M. Liang, "Fault diagnosis of wind turbine planetary gearbox under nonstationary conditions via adaptive optimal kernel time-frequency analysis," *Renew Energy*, vol. 66, pp. 468–477, Jan. 2014, doi: 10.1016/j.renene.2013.12.047.
- [11] N. Haloui, M. Abbas-Turki, and T. Rodet, "Robust fault detection for gearbox failure," in *2022 26th International Conference on System Theory, Control and Computing, ICSTCC 2022 - Proceedings*, Institute of Electrical and Electronics Engineers Inc., 2022, pp. 559–563. doi: 10.1109/ICSTCC55426.2022.9931829.
- [12] A. Soualhi, G. Clerc, and H. Razik, "Fault prognosis based on Hidden Markov Models," in *Proceedings - 2015 IEEE Workshop on Electrical Machines Design, Control and Diagnosis, WEMDCD 2015*, Institute of Electrical and Electronics Engineers Inc., Aug. 2015, pp. 271–278. doi: 10.1109/WEMDCD.2015.7194540.

- 
- [13] F. Ding, X. Wang, Q. Chen, and Y. Xiao, "Recursive Least Squares Parameter Estimation for a Class of Output Nonlinear Systems Based on the Model Decomposition," *Circuits Syst Signal Process*, vol. 35, no. 9, pp. 3323–3338, Sep. 2016, doi: 10.1007/s00034-015-0190-6.
- [14] W. Cui, M. Eng, and F. He, "Kalman Filter Based Fault Detection and Diagnosis," Flinders University 2018.
- [15] D. Zhao, W. Cheng, R. X. Gao, R. Yan, and P. Wang, "Generalized Vold-Kalman Filtering for Nonstationary Compound Faults Feature Extraction of Bearing and Gear," *IEEE Trans Instrum Meas*, vol. 69, no. 2, pp. 401–410, Feb. 2020, doi: 10.1109/TIM.2019.2903700.
- [16] J. Hu, S. Zheng, X. Liu, M. Wang, J. Deng, and F. Yan, "Optimizing the fault diagnosis and fault-tolerant control of selective catalytic reduction hydrothermal aging using the Unscented Kalman Filter observer," *Fuel*, vol. 288, Mar. 2021, doi: 10.1016/j.fuel.2020.119827.
- [17] I. Komorska, K. Olejarczyk, A. Puchalski, M. Wikło, and Z. Wołczyński, "Fault Diagnosing of Cycloidal Gear Reducer Using Statistical Features of Vibration Signal and Multifractal Spectra," *Sensors*, vol. 23, no. 3, Feb. 2023, doi: 10.3390/s23031645.
- [18] X. Zhang, J. Kang, L. Xiao, J. Zhao, and H. Teng, "A new improved Kurtogram and its application to bearing fault diagnosis," *Shock and Vibration*, vol. 2015, 2015, doi: 10.1155/2015/385412.
- [19] B. Li, M.-Y. Chow, Y. Tipsuwan, and J. C. Hung, "Neural-Network-Based Motor Rolling Bearing Fault Diagnosis," *IEEE Transactions on Industrial Electronics*, Vol. 47, no. 5, October 2000.
- [20] J. Y. Lee, "Sound and vibration signal analysis using improved short-time Fourier representation," *International Journal of Automotive and Mechanical Engineering*, vol. 7, no. 1, pp. 811–819, 2013, doi: 10.15282/ijame.7.2012.1.0066.
- [21] N. Haloui, D. Chikouche, and M. Benidir, "Diagnosis of Gear Systems by Spectral Analysis of Vibration Signals," *IJCSNS International Journal of Computer Science and Network Security*, vol. 7, no. 10, 2007.
- [22] L. Xu, T. Wang, J. Xie, J. Yang, and G. Gao, "A Mechanism-Based Automatic Fault Diagnosis Method for Gearboxes," *Sensors*, vol. 22, no. 23, Dec. 2022, doi: 10.3390/s22239150.
- [23] M. Saïd, N. Saïd, M. El, H. Benbouzid, and A. Benchaib, "Detection of Broken Bars in Induction Motors Using an Extended Kalman Filter for Rotor Resistance Sensorless Estimation," in *IEEE Transactions on Energy Conversion*, 2000, pp. 66–70.
- [24] Y. Sun, Y. Du, and Y. Zhang, "Fault Estimation Method for Nonlinear Systems With Perturbations Based on Augmented Fault Observer," *IEEE Access*, vol. 13, pp. 15301 – 15311, 2025, doi: 10.1109/ACCESS.2025.3531559.
- [25] D. Wang, "Hierarchical parameter estimation for a class of MIMO Hammerstein systems based on the reframed models," *Appl Math Lett*, vol. 57, pp. 13–19, Jul. 2016, doi: 10.1016/j.aml.2015.12.018.
- [26] C. Liu, S. Zhang, Z. Wang, F. Ma, and Z. Sha, "Research on Fault Prediction Method for Electric Multiple Unit Gearbox Based on Gated Recurrent Unit–Hidden Markov Model," *Applied Sciences (Switzerland)*, vol. 14, no. 12, Jun. 2024, doi: 10.3390/app14125320.
- [27] S. M. Kay and S. L. Marple, "Spectrum Analysis—A Modern Perspective," in *Proceedings of the IEEE*, 1981.
- [28] D. Bensaad, F. Guillet, and A. Soualhi, "Kurtosis analysis as cycle-ratio function in gear and bearing fault detection," *International Conference on Condition Monitoring and Machinery, Failure Prevention Technologies*, January 2016. [Online], <https://www.researchgate.net/publication/316715810>
- [29] Hafida Mahgoun, Rais Elhadi Bekka, Ahmed Felkaoui, "Gearbox fault detection using a new denoising method based on ensemble empirical mode decomposition and FFT," 4<sup>th</sup> International Conference on Integrity, Reliability and Failure, Funchal/Madeira, 23-27 June 2013.
- [30] Xining Zhang, Rongtong Zhou and Wenwen Zhang, "Improved local cepstrum and its applications for gearbox and rolling bearing fault detection," *Measurement Science and Technology*, Volume 30, Number 7, 7 June 2019, Doi: 10.1088/1361-6501.